

AD-A204 614

DTIC FILE COPY

4100 0500 0000 0000

(2)

MICROWAVE LABORATORY REPORT NO. 88-P-6

NONLINEAR ANALYSIS OF A MONOLITHIC QWITT
OSCILLATOR

TECHNICAL REPORT

AMIR MORTAZAWI, VIJAY KESAN, DEAN NEIKIRK AND
TATSUO ITOH

DECEMBER 1988

DTIC
SELECTED
FEB 22 1989
S D
C H

ARMY RESEARCH OFFICE
CONTRACT DAAL03-88-K-0005

JOINT SERVICES ELECTRONICS PROGRAM
RESEARCH CONTRACT AFOSR F49620-86-C-0045

THE UNIVERSITY OF TEXAS
DEPARTMENT OF ELECTRICAL ENGINEERING
AUSTIN, TEXAS 78712

DISTRIBUTION STATEMENT A

Approved for public release;
Distribution Unlimited

89 2 16 141

UNCLASSIFIED

SECURITY CLASSIFICATION OF THIS PAGE

MASTER COPY

ADA204614 FOR REPRODUCTION PURPOSES

REPORT DOCUMENTATION PAGE

1a. REPORT SECURITY CLASSIFICATION Unclassified		1b. RESTRICTIVE MARKINGS	
2a. SECURITY CLASSIFICATION AUTHORITY		3 DISTRIBUTION/AVAILABILITY OF REPORT Approved for public release; distribution unlimited.	
2b. DECLASSIFICATION/DOWNGRADING SCHEDULE		5 MONITORING ORGANIZATION REPORT NUMBER(S) ARO 25045.18-EL	
4. PERFORMING ORGANIZATION REPORT NUMBER(S) Microwave Laboratory Report Bi, 88-P-6		6a. NAME OF PERFORMING ORGANIZATION The University of Texas	
6b. OFFICE SYMBOL (If applicable)		7a. NAME OF MONITORING ORGANIZATION U. S. Army Research Office	
6c. ADDRESS (City, State, and ZIP Code) Dept. of Electrical & Computer Engineering Austin, Texas 78712		7b. ADDRESS (City, State, and ZIP Code) P. O. Box 12211 Research Triangle Park, NC 27709-2211	
8a. NAME OF FUNDING/SPONSORING ORGANIZATION U. S. Army Research Office		8b. OFFICE SYMBOL (If applicable)	
8c. ADDRESS (City, State, and ZIP Code) P. O. Box 12211 Research Triangle Park, NC 27709-2211		9 PROCUREMENT INSTRUMENT IDENTIFICATION NUMBER DAAK03-88-K-0005	
10 SOURCE OF FUNDING NUMBERS		PROGRAM ELEMENT NO	PROJECT NO
		TASK NO	WORK UNIT ACCESSION NO
11 TITLE (Include Security Classification) Nonlinear Analysis of a Monolithic QWITT Oscillator			
12 PERSONAL AUTHOR(S) Amir Mortazawi, Vijay Kesan, Dean Neikirk and Tatsuo Itoh			
13a. TYPE OF REPORT Technical	13b. TIME COVERED FROM _____ TO _____	14 DATE OF REPORT (Year, Month, Day)	15 PAGE COUNT
16. SUPPLEMENTARY NOTATION The view, opinions and/or findings contained in this report are those of the author(s) and should not be construed as an official Department of the Army position or policy, or decision, unless so designated by other document plan.			
17. COSATI CODES		18 SUBJECT TERMS (Continue on reverse if necessary and identify by block number) quantum well injection, transit time device, large signal mode, harmonic balance method, periodic loading, monolithic oscillator	
19 ABSTRACT (Continue on reverse if necessary and identify by block number) The small and large signal analysis of QWITT diode oscillators is presented. The small signal analysis determines the oscillation frequency of a power combining periodic structure. The large signal analysis, by the harmonic balance method, determines the power and efficiency of a single diode oscillator. These analyses show that the QWITT diode is a good candidate for signal generation in the millimeter wave region. The theoretical results predict that powers of about 1 mW can be obtained at frequencies up to 600 GHz. At the end experimental results are presented that confirm microwave operation of the QWITT device. The experiments have demonstrated powers of 300uW through the X-band.			
20. DISTRIBUTION/AVAILABILITY OF ABSTRACT <input type="checkbox"/> UNCLASSIFIED/UNLIMITED <input type="checkbox"/> SAME AS RPT <input type="checkbox"/> DTIC USERS		21 ABSTRACT SECURITY CLASSIFICATION Unclassified	
22a. NAME OF RESPONSIBLE INDIVIDUAL		22b. TELEPHONE (Include Area Code)	22c. OFFICE SYMBOL

MICROWAVE LABORATORY REPORT NO. 88-P-6

NONLINEAR ANALYSIS OF A MONOLITHIC QWITT
OSCILLATOR

TECHNICAL REPORT

AMIR MORTAZAWI, VIJAY KESAN, DEAN NEIKIRK AND
TATSUO ITOH

DECEMBER 1988

ARMY RESEARCH OFFICE
CONTRACT DAAL03-88-K-0005

JOINT SERVICES ELECTRONICS PROGRAM
RESEARCH CONTRACT AFOSR F49620-86-C-0045

THE UNIVERSITY OF TEXAS
DEPARTMENT OF ELECTRICAL ENGINEERING
AUSTIN, TEXAS 78712

ABSTRACT

The small and large signal analysis of QWITT diode oscillators is presented. The small signal analysis determines the oscillation frequency of a power combining periodic structure. The large signal analysis, by the harmonic balance method, determines the power and efficiency of a single diode oscillator. These analyses show that the QWITT diode is a good candidate for signal generation in the millimeter wave region. The theoretical results predict that powers of about 1 mW can be obtained at frequencies up to 600 GHz. At the end experimental results are presented that confirm microwave operation of the QWITT device. The experiments have demonstrated powers of 300 μ W through the X-band.



Accession For	
NTIS	GRA&I <input checked="" type="checkbox"/>
DTIC TAB	<input type="checkbox"/>
Unannounced	<input type="checkbox"/>
Justification _____	
By _____	
Distribution/ _____	
Availability Codes _____	
Dist	Avail and/or Special
A-1	

TABLE OF CONTENTS

Acknowledgment	iii
Abstract	iv
Table of Contents	v
Chapter 1- Introduction	1
Chapter 2- Small Signal Analysis	4
2.1- Analysis of the Structure	4
2.1.1- Calculation of the Post Impedance	5
2.1.2- Small Signal Modeling of the QWITT	8
2.1.3- Calculation of Complete Admittance	11
2.2- Analysis and Results	13
Chapter 3- Large Signal Analysis	15
3.1- Different Large Signal Analysis Schemes	15
3.1.1- Time Domain Analysis	15
3.1.2- Hybrid Analysis: Harmonic Balance Method	16
3.1.3- Volterra Series Approach	17
3.1.4- Voltage Update Method	18
3.2- The piecewise Harmonic Balance Method for	
Large Signal Analysis	18
3.2.1- Test 1: Van der Poll Oscillator	23
3.2.2- Test 2: Diode With Negative Conductance	28
3.2.2a- Estimation of the Amplitude and Frequency of Oscillation	31
3.2.2b- The Harmonic Balance Results	34

3.3- Large Signal Analysis of a QWITT Oscillator	38
3.3.1- Large Signal Model of the QWITT	38
3.3.2- Results of Harmonic Balance Analysis	42
Chapter 4- Experiment	45
4.1- Diode in Rectangular Waveguide	45
4.2- Planar Structure	47
Chapter 5- Conclusion	49
References	50

Chapter 1

INTRODUCTION

In recent years there has been a new interest in millimeter (mm) wave technology. Vacuum tube sources that cover the entire mm wave spectrum exist but there is a demand for solid state devices capable of operation at mm and sub mm wave frequencies. There are solid state sources such as IMPATT and GUNN diodes that can operate in the lower mm wave region but their efficiency and performance degrade at higher frequencies.

Quantum well devices have recently been shown to have a potential to generate mm and sub mm wave frequencies [1]. This is because the intrinsic negative resistance region for the quantum well device extends from dc up to several hundred GHz. One drawback of the quantum well device is its low output power. A new device, the quantum well injection and transit time (QWITT) diode was proposed. This device exploits transit time phenomena to improve the output power of the conventional quantum well devices. Quantum well oscillators are also very attractive because they are intrinsically very low noise. In order to generate higher output power in the mm wave region, different power combining techniques can be used.

Ordinarily a real physical system is a nonlinear function of its operating parameters; therefore, if a complete and accurate analysis of the system is desirable the nonlinear equations representing the physical problem should be solved. Since the task of solving the nonlinear equations is often very difficult, it is necessary to simplify a nonlinear problem through some assumptions. After the design work is done the system can be built. If it does not have all the desirable characteristics, one can achieve

the final design by trial and error. Depending on the type of system, the designer can impose some restrictions on the operating condition of that system so then its operation in a linear region is ensured. In this case small signal analysis is satisfactory.

An oscillator relies on device nonlinearity for proper operation and is inherently a nonlinear system. Due to nonlinear operation often higher order harmonics are generated that effect the frequency of oscillation, the power generated and the efficiency of the oscillator. It is only by nonlinear analysis that one can determine the exact frequency of operation, the power and efficiency of the oscillator, the power of undesirable higher harmonics relative to the power generated at the fundamental frequency, and the limitations of a microwave oscillator. Another important fact that makes nonlinear analysis necessary is the design of monolithic microwave integrated circuits (MMIC). The opportunity of trimming a circuit after design is not available in the case of MMICs and redesigning and reproducing them is very time consuming and costly. Therefore, it is very desirable to be able to design and construct an MMIC circuit which meets all the specifications without going through any trial and error. The nonlinear analysis of a circuit helps the design engineer to achieve this goal.

A complete analysis of a nonlinear circuit requires a nonlinear device model and analytic means to extract the effect of device-circuit interactions from the model. There exist different methods to solve nonlinear problems. In general one can write a set of nonlinear differential equations to represent a dynamical system. In principle, the analysis can be performed by integrating the system's differential equations. If it is desired to find the steady state response of a circuit as it is in the case of oscillators, it is necessary to carry out the integration till the transient responses die out. This approach is prohibitively expensive whenever the transients are governed by time constants that

are very much larger than the period of the driving force of an amplifier or the oscillation of an oscillator. In this case, continuous integration may have to be carried out for hundreds of full periods before the transients become small enough to ignore. A better method to analyze this type of problems is the harmonic balance technique [2]. In the harmonic balance method, each state variable is represented by a Fourier series that satisfies the requirement of periodicity. An optimization algorithm is then used to adjust the coefficients of the Fourier series such that the system equations are satisfied with least square error.

In this work a small signal and large signal analysis of a single QWITT diode and also a small signal analysis of a power combining structure are performed. At the end some experimental work is done and experimental and theoretical data are compared.

Chapter 2

SMALL SIGNAL ANALYSIS

In order to realize a planar QWITT diode oscillator one can insert a QWITT diode via an inductive post inside a parallel-plate waveguide. This type of configuration is convenient for design of monolithic microwave integrated circuits (MMIC) in the mm wave region.

To obtain higher output power at mm wave frequencies a TEM parallel-plate waveguide can be loaded periodically with QWITT diodes. This simple design includes a resonant circuit which when properly designed precludes the need for any external resonant circuitry.

2.1 - Analysis of The Structure

The parallel-plate waveguide loaded periodically with QWITT diodes is shown in Fig.(2-1). The waveguide is open on one end and terminated by a resistive load at the other end. Assuming that we are given the small signal impedance of the QWITT diode at a particular frequency (f_r) our objective is to design a periodic QWITT diode oscillator to oscillate at the frequency f_r . The parameters that should be determined are the width (w), the height (b) of the waveguide, the distance between the load and the metallic post (d_{in}), the length of the open part of the waveguide (d_{out}), the periodicity of the structure (d) (in the case of having more than one diode mounted inside the waveguide) and the impedance of the load (Z_l).

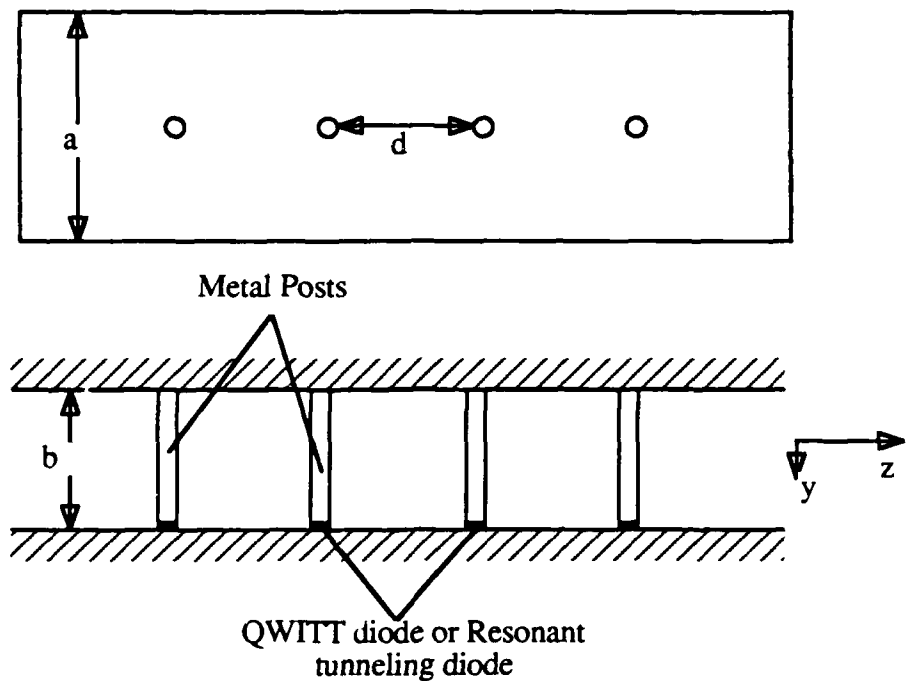


Fig.(2-1): schematic representation showing top and side views of parallel plate waveguide periodically loaded by QWITT diodes

2.1.1 - Calculation of The Post Impedance:

The parallel plate waveguide loaded periodically with the QWITT diodes is modeled by an equivalent transmission line loaded periodically with the impedance Z_p . The impedance Z_p is the sum of the small signal impedance of the QWITT diode and the metal post reactance. Here we treat the QWITT diode as a lumped element, and the electric field component and the current density are assumed to be oriented in the Y direction (Fig.2-1(b))

The small signal impedance of the diode and the metal-post reactance need to be calculated. Since the thickness of the QWITT diode is much smaller than the length of the supporting metal post, we can not neglect the effect of the reactance of the post.

The mode-matching technique can be used to calculate the first-order inductance of the post [3-4]. The cross sectional view of the waveguide modeled is shown in Fig.(2-2).

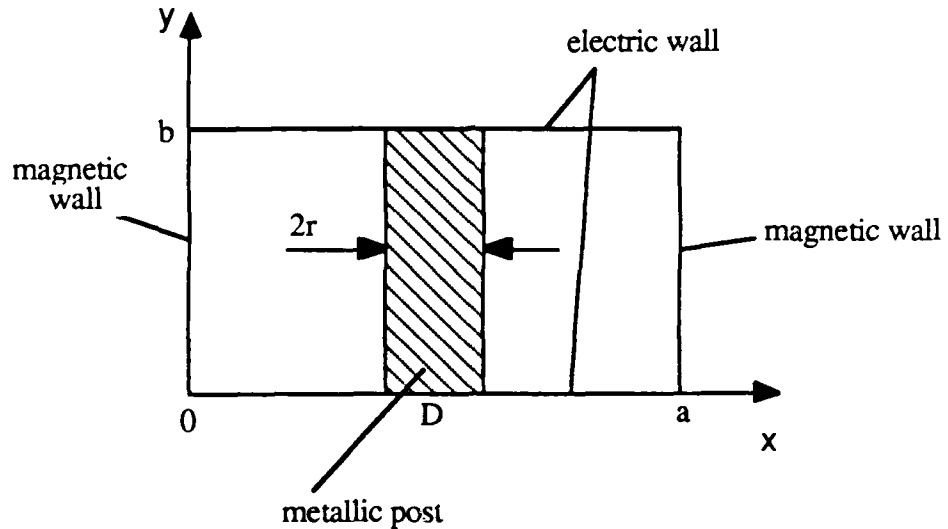


Fig.(2-2): Cross sectional view of the analytical model for the calculation of the metal post reactance

The impedance of the post jX_o can be obtained by the following formula.

$$X_o = \frac{k}{4} \left(\frac{-a}{\pi} \log \left(4 \sin \left(\frac{\pi r}{2a} \right) \sin \left(\frac{\pi D}{a} \right) \right) + \sum_{m=1}^{\infty} \left(1 + \cos \frac{2m\pi D}{a} \right) \left(\frac{1}{\gamma_m} - \frac{a}{m\pi} \right) \right) \quad (2-1)$$

Consider that X_o is the normalized reactance of the post with respect to the characteristic impedance of the parallel-plate waveguide. The above formula is valid if the diameter of the post is much smaller than the width of the parallel plate waveguide. If the post is located at the center of the waveguide ($D = \frac{a}{2}$), then:

$$X_o = \frac{k}{4} \left\{ \frac{-a}{\pi} \log\left(\frac{2\pi r}{a}\right) + \sum_{m=2,4,\dots}^{\infty} 2 \left(\frac{1}{\gamma_m} - \frac{a}{m\pi} \right) \right\} \quad (2-2)$$

where

$$\gamma_m = \sqrt{\left(\frac{m\pi}{a}\right)^2 - K^2} \quad (2-3)$$

and

$$K = \sqrt{\epsilon_r} K_o \quad (2-4)$$

and

$$K_o = \frac{2\pi}{\lambda} = \frac{2\pi f}{c} = 2\pi f \sqrt{\mu_0 \epsilon_0} \quad (2-5)$$

The total post impedance, Z_p , is the characteristic impedance of the QWITT and the post reactance is given by :

$$Z_p = Z_{\text{diode}} + j Z_o X_o \quad (2-6)$$

where Z_o is the characteristic impedance of the parallel-plate waveguide. Since the parallel-plate waveguide is modeled as a TEM transmission line then referring to Fig.(2-3) we can write:

$$V = E b \quad (2-7)$$

and

$$I = H a \quad (2-8)$$

then

$$Z_o = \frac{V}{I} = \frac{E b}{H a} = \eta \frac{b}{a} \quad (2-9)$$

$$\eta = \frac{\eta_0}{\sqrt{\epsilon_r}} \quad (2-10)$$

and

$$\eta_0 = 120 \pi \quad (2-11)$$

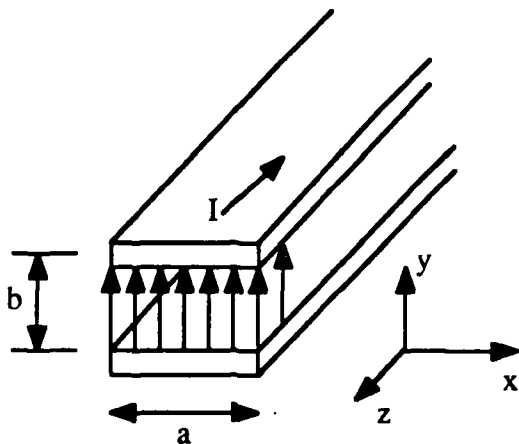


Fig.(2-3): TEM model of a parallel plate waveguide

where ϵ_r is the relative dielectric constant of the medium inside the parallel plate waveguide. The above formula is valid when the width of the parallel-plate waveguide is much larger than its height ($a \gg b$).

2.1.2 - Small Signal Modeling of The QWITT

The physical structure of the QWITT diode consists of a single GaAs quantum well sandwiched between two thin layers of $\text{Al}_x\text{Ga}_{1-x}\text{As}$, together with a drift region of undoped GaAs [5]. This structure is then placed between two n^+ GaAs regions to form contacts (Fig. 2-4)

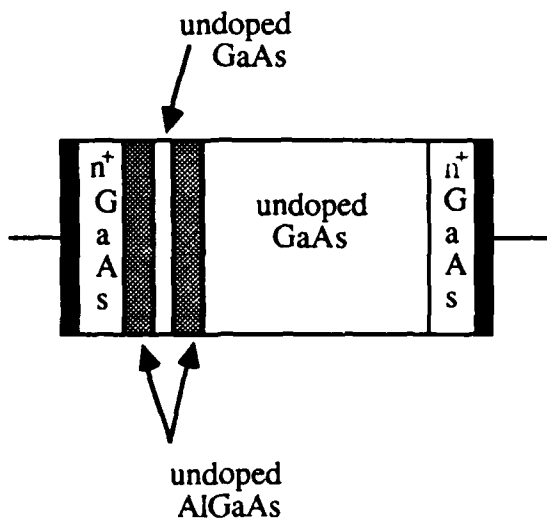


Fig.(2-4): Phsical structure of the QWITT diode

The small signal equivalent circuit of the QWITT is shown in Fig.(2-5).

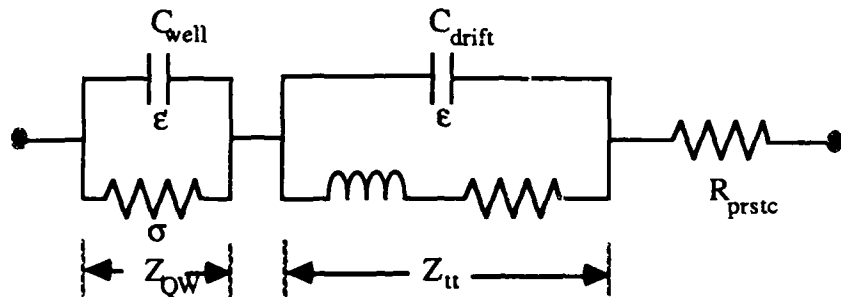


Fig.(2-5):QWITT's equivalent circuit

It is assumed that the length of the quantum well region "l" is much smaller than the depleted spacer layers W. The specific impedance of the quantum well injection at an angular frequency ω is then given by

$$Z_{\text{QW}} = \frac{1}{\sigma + j\omega\epsilon'} \quad (2-12)$$

where ϵ' is the effective dielectric constant of the injection region and σ is the normalized injection conductance. The total small signal specific impedance (excluding parasitic elements) of the QWITT diode is the sum of this specific impedance and that of the depleted spacer region Z_u .

$$Z = Z_{QW} + Z_u \quad (2-13)$$

Based on the frequency-independent injection conductance and the constant saturation velocity the drift region electric field can be integrated to obtain the specific impedance at an angular frequency ω for the QWITT device as

$$Z_u = \frac{W}{j\omega\epsilon} \left[1 - \frac{\sigma}{\sigma+j\omega\epsilon} \frac{1-\exp(-j\theta_d)}{j\theta_d} \right] \quad (2-14)$$

where ϵ is the dielectric constant of the drift region and θ_d is the drift angle given by:

$$\theta_d = \frac{\omega W}{v_s} \quad (2-15)$$

The real part of Eq.(2-14) gives the negative resistance obtained from the depleted spacer region as:

$$R = \frac{2 \left(\frac{v_s \epsilon}{2\sigma^2} \right)}{\left(\frac{\omega}{\sigma/\epsilon} \right)^2 \left[1 + \left(\frac{\omega}{\sigma/\epsilon} \right)^2 \right]} \left[1 - \cos\left(\frac{\omega W}{v_s}\right) + \frac{\omega}{\sigma/\epsilon} \sin\left(\frac{\omega W}{v_s}\right) \right] \quad (2-16)$$

The specific resistance of the quantum well injection region is given by the real part of Eq.(2-12)

$$R_{QW} = \frac{\frac{1}{\sigma}}{1 + \left(\frac{\omega}{\sigma/\epsilon}\right)^2} \quad (2-17)$$

The total specific resistance of a QWITT diode (excluding parasitic resistance in the device) is given by the sum of Eqs (2-16) and (2-17).

2.1.3 - Calculation Of Complete Admittance

Based on the last two sections we can determine the value of the loaded impedance Z_p which is the sum of the QWITT diode small signal impedance and the reactance of the post. The periodic structure is shown in Fig.(2-6).

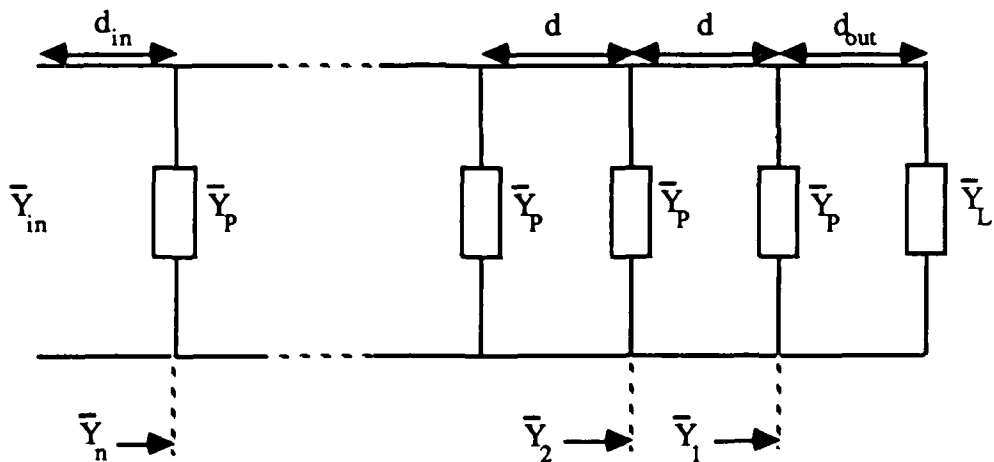


Fig.(2-6): Transmission line model of the finite length periodic QWITT oscillator

The characteristics of this structure can be found using the theory of periodic structures; however, a different approach can be used. In practice it is not necessary to have many diodes and it is desirable to keep the total line length short to ensure operation at only one frequency. That is, the separation of the resonant frequencies becomes large as the length decreases. As shown in Fig.(2-6), simple admittance transforms can be used to analyze the periodic structure.

$$\begin{aligned}\bar{Y}_1 &= \frac{\bar{Y}_L + \tanh(\gamma d_{out})}{1 + \bar{Y}_L \tanh(\gamma d_{out})} + \bar{Y}_P \\ \bar{Y}_2 &= \frac{\bar{Y}_1 + \tanh(\gamma d)}{1 + \bar{Y}_1 \tanh(\gamma d)} + \bar{Y}_P \\ &\dots \\ &\dots \\ \bar{Y}_{in} &= \frac{\bar{Y}_n + \tanh(\gamma d_{in})}{1 + \bar{Y}_n \tanh(\gamma d_{in})} \quad (2-18)\end{aligned}$$

Where \bar{Y} is the impedance normalized to the characteristic impedance of the waveguide.

If we cut the circuit in two sections at any point, in order to satisfy the resonance condition the impedance looking in one direction should be equal to the negative of the impedance looking in the other direction. In our analysis first we assume that the two ends of the periodic structure are open circuited and since we transform all the impedances to the one end, the device should oscillate at the frequency where the imaginary part of the input admittance Y_{in} becomes zero. The conductance of the load is the negative of the real part of Y_{in} (Imaginary of $Y_{in} = 0.0$) Therefore by

connecting a load with resistance $\frac{1}{Y_{in}}$ to one end of the parallel plate waveguide the oscillation condition is satisfied.

2.2 Analysis and Results

As an illustration, a parallel-plate waveguide loaded with four QWITT diodes has been chosen. The dimensions of the waveguide and the QWITT diode parameters designed to operate at 94 GHz are as follows:

Width of the waveguide (a) = 254 μm

Thickness of the waveguide (b) = 25.4 μm

Distance between the diodes (d) = 866 μm

Diameter of the metal post and the diode = 25.4 μm

The waveguide is assumed to be filled with polyimide ($\epsilon_r=3.4$) and the waveguide terminations are assumed to be open circuited [6]. The physical parameters of the waveguide should permit monolithic circuit fabrication technology. The calculated input admittance as a function of frequency is shown in Fig.(2-7).

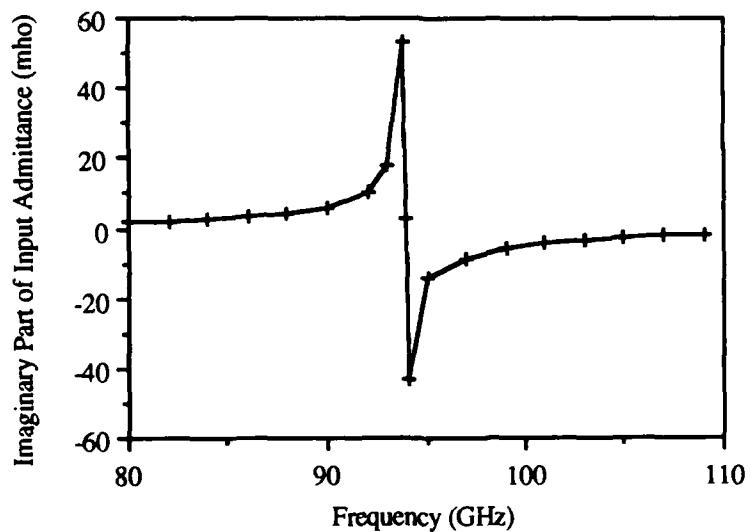


Fig.(2-7): Imaginary part of the input admittance versus frequency

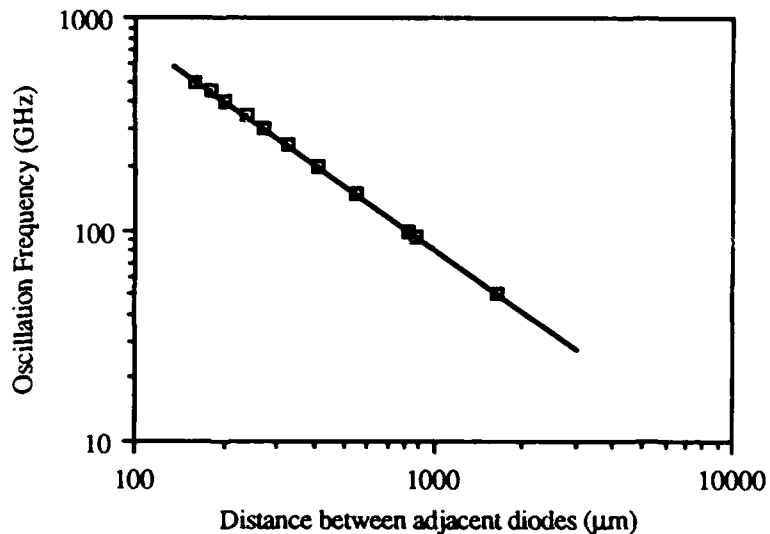


Fig.(2-8): Dependence of the oscillation frequency to the structure periodicity

Maintaining all diode and circuit parameters the same as those at 94 GHz, the distance, d , between the diodes is varied to obtain other resonant frequencies. At any desired operating frequency, the distance between the diodes must be equal to half the guide wavelength. Thus as the oscillation frequency is increased, the the distance between the diodes deceases as $1/f$ (Fig.2-8). The analysis also shows how variation in the width and thickness of the waveguide affects the oscillation frequency of the circuit designed to operate at 94 GHz. A deviation in width or thickness of the waveguide by even a factor of four causes less than 1% change in the oscillation frequency. Hence, the width and thickness of the waveguide, which determine its characteristic impedance, do not affect the oscillation frequency significantly. This is a distinct advantage from a circuit fabrication point of view.

Chapter 3

LARGE SIGNAL ANALYSIS

The optimum design of microwave circuits containing solid state devices requires an accurate technique for predicting their nonlinear performance. Designs based on small-signal parameters can roughly estimate the frequency, but not the power, the harmonic content, or the efficiency. There are many methods of nonlinear analysis, each one having its own specific features which should be considered based on the circuit to be analyzed and the desired results. Some methods are better for transient analysis, others for steady state response, some give faster results and some give more exact results but are very slow.

3.1 - Different Large Signal Analysis Schemes:

The analysis methods may be divided into four categories [7]

- 1) Time domain and direct integration methods: for transient and steady state analysis.
- 2) Hybrid analysis using time and frequency domain analysis together: for steady state analysis.
- 3) Nonlinear transfer functions: for weakly nonlinear circuit analysis.
- 4) Voltage update method: for steady state analysis of a nonlinear network excited by a sinusoidal source.

3.1.1 - Time Domain Analysis:

Time domain analysis requires solving a set of nonlinear integro-differential equations. Numerical integration techniques can be used to solve a nonlinear system of equations representing a dynamical system by applying appropriate initial conditions.

If the steady state solution is desired, numerical integration should be performed over many cycles till the transients die out. If the solution contains slow transients, the computation time can be overwhelmingly long. This is often the case for high Q circuits such as cavity stabilized oscillators. In general the time domain approach requires extensive computation time.

3.1.2 - Hybrid Analysis: Harmonic Balance Method

In the harmonic balance method [8] the periodic or quasi periodic steady state solution is obtained by solving the nonlinear differential equations representing the circuit in the frequency domain. This is carried out by considering as unknowns of the analysis problem the harmonic components V_k , I_k of the Fourier series which are used to expand all the variables in the circuit (e.g. the voltages v and the currents i) Eq.(3-1).

$$v(t) = \sum_{k=0}^m \operatorname{Re}[V_k e^{j\omega_k t}]$$

$$i(t) = \sum_{k=0}^m \operatorname{Re}[I_k e^{j\omega_k t}] \quad (3-1)$$

where ω_k is the angular frequency of the k^{th} spectral component and m is the number of harmonics needed for an adequate approximation of the solution. An optimization algorithm is used to adjust the coefficients of the Fourier series such that the system of equations is satisfied with least square error. Although the harmonic balance method avoids the computationally expensive process of numerically integrating the dynamic equations, its main disadvantage is the large number of variables that must be optimized.

3.1.3 - Volterra Series Approach

When the circuit to be analyzed is weakly nonlinear, an approximated steady-state solution can be obtained by Volterra series. The input-output relation for such nonlinear circuits can be viewed as a generalization of the convolution integral theorem in the analysis of linear circuits. If $x(t)$ is the input to a linear system, $h(t)$ is its impulse response and $y(t)$ is its output, then:

$$Y(t) = \int_0^t X(\tau) h(t-\tau) d\tau = \int_0^t X(t-\tau) h(\tau) d\tau \quad (3-2)$$

In the case of a nonlinear system the input-output behavior can be described by the Volterra functional expansion [9].

$$Y(t) = h_0(t) + \int_0^t h_1(t-\tau_1) X(\tau_1) d\tau_1 + \dots + \int_0^t \int_0^{\tau_1} \dots \int_0^{\tau_{n-1}} h_n(t-\tau_1, t-\tau_2, \dots, t-\tau_n) \\ X(\tau_1) X(\tau_2) \dots X(\tau_n) d\tau_1 d\tau_2 \dots d\tau_n \quad (3-3)$$

where $h_n(t, t_1, \dots, t_n)$ is called the nonlinear impulse response of order n . Its Fourier transform $H_n(f_1, f_2, \dots, f_n)$ can then be called the nonlinear transfer function of order n . In order to analyze a nonlinear circuit by means of Volterra series, it is necessary to calculate the nonlinear transfer functions H_1, H_2, \dots, H_n . As in any series expansion, this approximation is useful when the number of terms required for an adequate approximation to $y(t)$ is not very large. This is why the Volterra series approach is often used to analyze the systems with a weak nonlinearity.

3.1.4 - Voltage Update Method

This method is applicable to the analysis of a circuit containing linear and nonlinear elements which is excited by a sinusoidal source $E(t)$ [10]. Like the harmonic balance method the circuit is divided into two parts; one contains nonlinear elements (as well as some linear elements if necessary) and the other part; contains the remaining linear elements and the exciting source. The analysis starts with selection of an estimated value of voltage across the terminal connecting the linear and the nonlinear section $V_0^N(t)$; this value is usually taken at the exciting frequency, without harmonics. Using $V_0^N(t)$, the current in the nonlinear circuit $I_0^N(t)$ is found. Putting $I_0^l(t) = -I_0^N(t)$, the fast Fourier transform can be used to obtain $I_0^l(\omega)$ which is applied to the linear circuit. $V_0^L(\omega)$ is found by superposition. Then using an inverse Fourier transform we form $V_0^L(t)$ and compare it with initial $V_0^N(t)$. If the difference is significant, the iteration proceeds with a new estimate $V_1^N(t)$, and continues until the difference is significant.

3.2 - The Piecewise Harmonic Balance Method For Large Signal Analysis

Although the harmonic balance method avoids the computationally expensive process of numerically integrating the dynamic equations, its main disadvantage is the large number of variables that must be optimized. If the system of equations contains n state variables and each of them requires $2m+1$ Fourier coefficients (for the dc component and m harmonics), then there will be $n(2m+1)$ variables to be adjusted by the optimization routine. This makes the method impractical for large systems, unless a way is found to reduce the number of optimized variables. In order to reduce the complexity of the problem, a piecewise harmonic balance method [2] can be used. This method is essentially an harmonic balance technique with the advantage that it takes into

account the fact that considerable part of the network is usually linear. In this method not all the electrical variables in the circuit (e.g. nodal voltages and/or branch currents), but only those relative to the nonlinear components are dealt with as unknowns. This is used to reduce the number of optimized variables.

The piecewise harmonic balance method may be described by the following steps:

- 1) The nonlinear network under consideration is decomposed to a minimum possible number of linear sub-networks and a minimum number of nonlinear ones.(Fig.3-1).
- 2) The terminals of the linear sub networks are excited by periodic sources in the form of Fourier expansions.
- 3) Through the solution of the linear sub-networks in the frequency domain and by a suitable optimization routine, the coefficients of the Fourier series are adjusted so that the equations representing both the linear and the nonlinear sub-networks are satisfied.

After partitioning the circuit into linear and nonlinear sub-networks as shown in Fig.(3-1) (i.e. by putting only the intrinsically nonlinear components into the nonlinear blocks), only electrical variables at the connection ports have to be considered as unknowns of the harmonic balance problem.

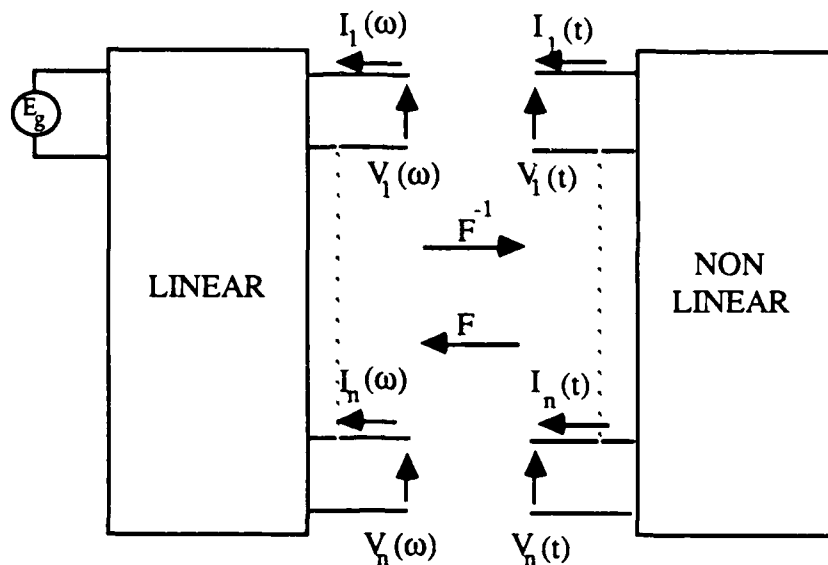


Fig.(3-1): Division of the circuit into linear and nonlinear sections

The linear sub-network response at the connection ports is obtained in the frequency domain by the set of equations:

$$A_k V_k + B_k I_k = C_k \quad \text{for } k=0, \dots, m \quad (3-4)$$

where V_k and I_k are the column vectors of the k^{th} spectral components of the n voltages and currents at the connection ports; A_k and B_k are determined by the linear network and C_k represents the excitation terms.

The nonlinear sub-network can be described by n nonlinear time-domain equations. In the case of a simple resistive voltage-controlled nonlinear elements it can be written as:

$$i = f(v) \quad (3-5)$$

or, in the case of a nonlinear element for which charge storage effects should also be taken into account, it takes the form

$$i = f(v, v') \quad (3-6)$$

where v' is the time derivative of voltage. In the more general case for complex nonlinear devices, the nonlinear equation has the form

$$f(v, \dot{v}, \dots, \overset{r}{v}, i, \dot{i}, \dots, \overset{s}{i}) = 0 \quad (3-7)$$

The nonlinear analysis consists of searching for those V_k, I_k which satisfy (by taking into account Fourier series Eq. 3-1) both the linear frequency domain Eq.(3-4) and the nonlinear time domain Eq.(3-7). Once the harmonic balance problem has been solved, all the other variables of the circuit can be determined by solving linear sub-network equations in the frequency domain. Eq.(3-4) can be written in the form

$$V_k = Z_k I_k + E_k \quad \text{for } k=0, \dots, m \quad (3-8)$$

By transforming this into time domain and substituting it into Eq.(3-7) we get a set of time-dependent equations

$$g(I_0, \dots, I_k, \dots, I_m, t) = 0 \quad \text{for } -T/2 \leq t \leq T/2 \quad (3-9)$$

where T is the period of the circuit response. In the case of quasi-periodic operation T goes to infinity.

Since the variables $v(t)$, $i(t)$ have been approximated by a Fourier series with a finite number of terms (m), it is not generally possible to find a set of harmonic components I_0, \dots, I_m of the currents which exactly satisfy Eq.(3-9) for every t , but only an approximate solution which gives the minimum discrepancy in Eq.(3-9). The minimum discrepancy criterion can be defined in different ways, and in particular, by the least-square error function.

$$EF(I_0, \dots, I_k, \dots, I_m) = \sum_{l=1}^n \frac{1}{T} \int_{-T/2}^{T/2} g_n^2(I_0, \dots, I_k, \dots, I_m, t) dt \quad (3-10)$$

Therefore the best approximated solution to the harmonic balance problem can be computed by finding harmonic components I_0, \dots, I_m of the currents which minimize EF by means of a numerical optimization algorithm. It should be noted that we could optimize coefficients of Fourier series for voltage wave forms at each interconnection instead of current wave forms as in the above case.

In the analysis of oscillators, it is also necessary to consider as unknown the period of the circuit response. In this case the unknown variables of the optimization problem are not only I_0, \dots, I_m but also the period T .

When the least square approximation criterion is used to define the error function, a general purpose numerical optimization algorithm such as a quasi Newton gradient method can be used to minimize the error function.

In the harmonic balance technique there is always a need for a suitable initial estimate for the solution. This initial estimate strongly affects the convergence

characteristics of the optimization procedure. Since in practice it is very difficult to estimate the unknown harmonic components of the variables, convergence problems would be encountered in strongly nonlinear circuits, unless suitable strategies were adopted. One way is to start from small values of the excitation terms, so that nonlinear effects are not strong, then increase their amplitude gradually in successive steps, till the nominal values are reached. At every step the solutions found in previous steps are used as initial estimate for the iterative analysis algorithm. (It should be considered that the above can not be applied to the case of oscillator analysis.)

Since we are interested only in the steady state analysis of microwave oscillators, the harmonic balance seems to be the proper method of analysis. For the optimization part a general purpose optimization routine from the IMSL library (UMINF) can be used. The subroutine NONLINEAR in our program contains the nonlinear device model. By modifying this subroutine different devices can be used as the nonlinear part of the oscillator circuit. In order to test the convergence behavior of the nonlinear analysis program two different test problems are solved. This helps us to investigate the performance of the optimization routine and study the sensitivity of convergence to the initial guess.

3.2.1 - Test 1: Van der Pol Oscillator

Van der Pol's equation seems to be a classical example of a nonlinear oscillatory system. It is of the form

$$\begin{aligned}\dot{X}_1 &= X_2 \\ \dot{X}_2 &= \mu(1 - X_1^2)X_2 - X_1\end{aligned}\tag{3-11}$$

The network realization of Van der Pol's equation is shown in Fig.(3-2)

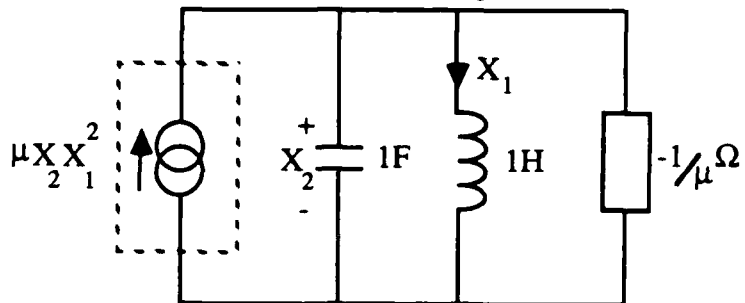


Fig.(3-2): Circuit representation of the Van der Pol's oscillator

The factor μ determines the amount of nonlinearity. If μ is very small, the term $\mu(1 - X_1^2)$ can be neglected. In this case the differential equation represents a simple harmonic oscillatory system which consists of a 1 F capacitor in parallel with a 1 H inductor. In this case the period of oscillation is 2π . If on the other hand μ is not small, because of nonlinearity effects, the oscillation waveform will contain higher harmonics. Harmonic contents cause the period of oscillation to increase slightly. This is because the voltage is not a single harmonic any more. Acting with the nonlinear element, it produces a current which is far from a simple sinusoid. One component of this current is at the fundamental frequency. The frequency must be such that the fundamental current multiplied by the impedance of the LC circuit at this frequency gives the fundamental voltage. This condition requires that the resonance frequency of the oscillation be slightly lower than the resonance frequency of the LC circuit.[11] In this analysis we choose $\mu=1$ (strong nonlinearity).

In order to analyze the circuit using the harmonic balance method, the circuit is divided into nonlinear and linear subcircuits. The nonlinear subcircuit is shown by the dashed lines (Fig.3-2). For the analysis we assume the linear and the nonlinear

subcircuits are excited by a voltage source $V(f_1 \dots f_m)$ which contains m harmonics. For the steady state resonance condition to be satisfied, the impedance looking into the nonlinear element should be equal to the negative of the impedance seen from the linear subcircuit port. Therefore if the voltage V is equal to the true steady state voltage which should appear across the linear and nonlinear subcircuit's terminals, the sum of the currents flowing into the linear and nonlinear subcircuits should be equal to zero.

The nonlinear analysis program requires an initial guess (V_g) for the voltage V . Generally the initial guess contains an approximate value for the frequency and amplitude of the fundamental oscillation (it can also contain amplitude and phase of the higher harmonics). Then the current flowing into the linear circuit ($I_{\text{linear}}(f_1 \dots f_m)$, m' can vary between 1 to m depending on the number of harmonics in the initial guess) is calculated in the frequency domain. After sampling the voltage V_g in the time domain, the current through the nonlinear element is determined ($I_{\text{nonlinear}}(t)$). Through an iterative procedure using the optimization routine frequency, amplitudes and phases of the n harmonics of the voltage (V_g) can be chosen such that an error function defined as r.m.s value of the sum of currents through the linear and the nonlinear subcircuits is minimized. The voltage waveform V_g that minimizes the error function is the steady state solution to the problem. Since the current through the linear circuit is in the frequency domain and the current through the nonlinear circuit is in the time domain, one can define the error function in the time (by transferring $I_{\text{linear}}(f_1 \dots f_m)$ to the time domain) or in the frequency domain (by transferring $I_{\text{nonlinear}}(t)$ to the frequency domain using an FFT algorithm). The error function in the time domain is given by

$$EF_t = \sum_{t=t_1, t_2}^T (I_{\text{linear}}(t) + I_{\text{nonlinear}}(t))^2 \quad (3-12)$$

where T is the period of oscillation and t_1, t_2, \dots are the sampling points.

The error function in the frequency domain is given by

$$EF_f = \sum_{l=1,2..}^m (I_{\text{linear}}(f_l) + I_{\text{nonlinear}}(f_l))^2 \quad (3-13)$$

where m is the number of harmonics considered in the analysis. Either of the two error functions can be used in the optimization procedure, but as presented below, different performance is observed with the two different error functions.

The sensitivity to the initial guess of the program using Erf_f is less even though the program takes a longer time to converge. Results of several runs containing the initial guess and the final values after convergence are given below. After each result the wave form across the nonlinear device's terminals is plotted. The period and amplitude of the waveform is very close to the one calculated by Nakhla [2].

Initial guess:

amplitude of the first harmonic: 2.0

phase: 0

period of oscillation: 5.0

Final value:

period of oscillation: 6.6645s

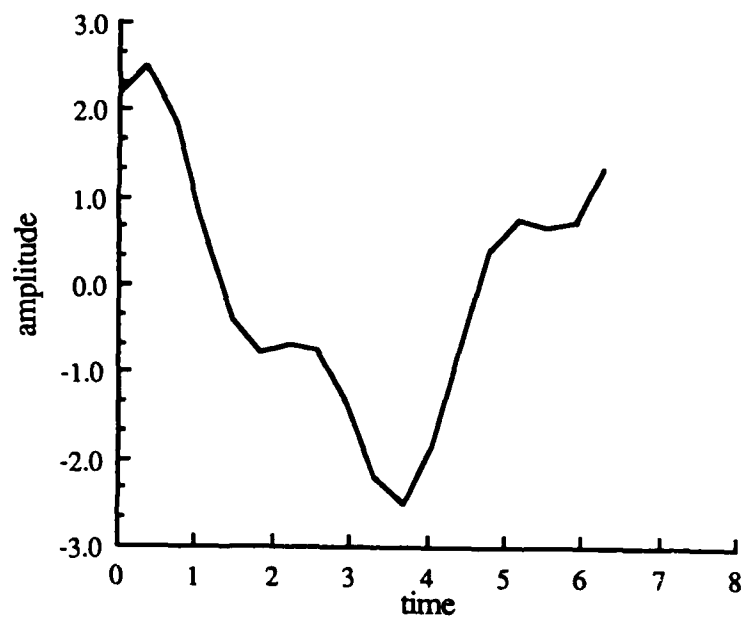


Fig.(3-3): The amplitude of voltage for three harmonic components

final value: period of oscillation: 6.6635 s

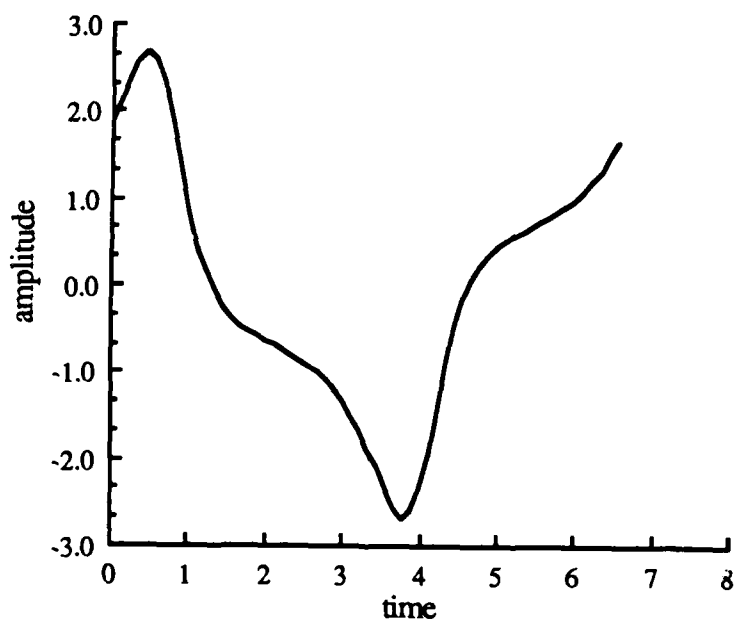


Fig.(3-4): the amplitude of voltage with ten harmonic components

The nonlinear analysis program which uses the error function in the frequency domain is less sensitive to the initial guess.

3.2.2 - Test 2: Diode With Negative Conductance

To test the nonlinear analysis program again the large signal analysis of a negative resistance diode oscillator is performed. The negative resistance diode is inserted in a parallel plate waveguide via an inductive post.

The diode has a negative dynamic conductance which is obtained by application of a proper bias voltage. Some examples of negative conductance diodes are IMPATT, Tunnel, TRAPATT and QWITT diodes. As a first approximation, the frequency dependence of the negative conductance may be neglected as long as the frequency range over which the diode operates is small enough. The negative conductance may be represented in the frequency range which the above approximation is valid, by a function relating high frequency current to voltage. This function is nonlinear for large signals applied across the diode's terminals. This nonlinear relation may be approximated by a cubic function shown in Fig.(3-5).[12]

If the operation point is assumed to be the origin of the coordinate system, the instantaneous value of the current given by:

$$I = -a_1 V + a_3 V^3 \quad (3-14)$$

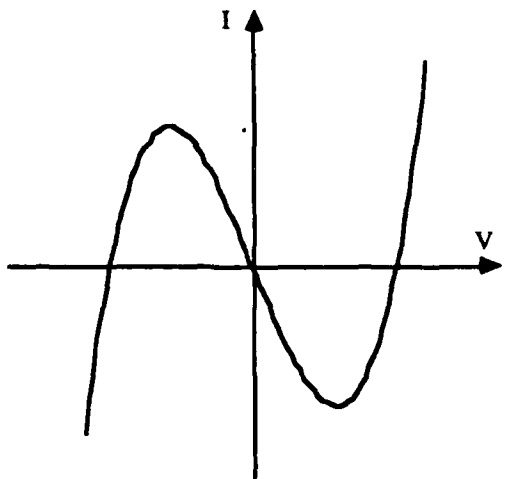


Fig.(3-5): cubic approximating curve

The dynamic conductance is the derivative of the current with respect to the voltage. It is given by:

$$G = -a_1 + 3a_3 V^2 \quad (3.15)$$

This shows that as the instantaneous value of the voltage across the diode increases the dynamic negative conductance of the diode decreases. The equivalent circuit of the negative conductance diode is shown in Fig.(3-6)

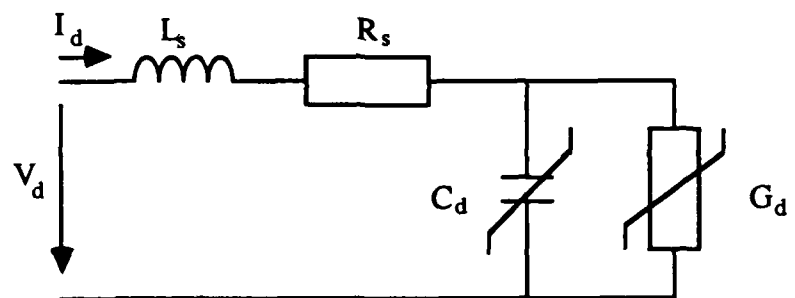


Fig.(3-6): Equivalent circuit of a negative resistance diode

The negative conductance (G_d) is shunted by the junction capacitance (C_d). L_s and R_s are series inductance and resistance respectively.

Both the diode's negative conductance and junction capacitance are assumed to be frequency independent. The diode's negative conductance may be expressed as

$$G_d = -G_o(1 - \alpha V_o^2) \quad (3-16)$$

where G_d is the r.m.s negative conductance of the diode, G_o is the negative value of the diode small signal conductance, α is a diode parameter which can be determined by measurements on an oscillating diode and V_o is the r.m.s value of the voltage across the diode. The comparison of Eq.(3-14) and Eq.(3-16) results in

$$G_o = a_1 \quad (3-17)$$

$$\alpha = \frac{3}{2} \frac{a_3}{a_1} \quad (3-18)$$

The level dependence of the junction capacitance may be approximated by an expression similar to that giving the level dependence of the conductance.

$$C_d = C_{do}(1 + \beta V_o^2) \quad (3-19)$$

Where β is a diode parameter. The impedance across the diode's terminals is given by:

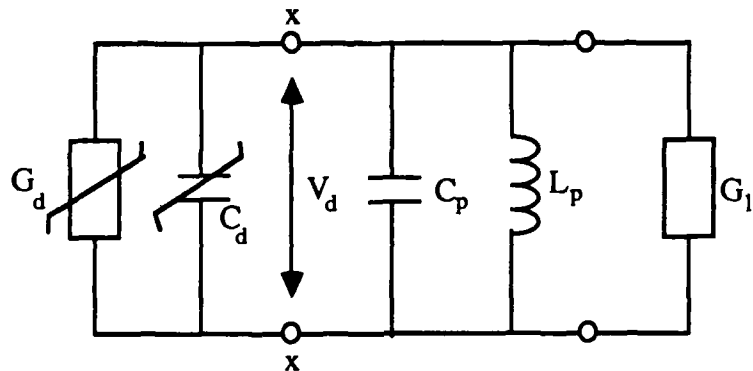
$$Z = \frac{G_d + j\omega C_d}{G_d^2 + \omega^2 C_d^2} + R_s + j\omega L_s \quad (3-20)$$

The impedance is dependent on the amplitude of the voltage across the diode because G_d and C_d are dependent on it. Due to the junction capacitance and series resistance, the negative conductance of the diode decreases with increasing frequency even though the junction conductance G_d is assumed to be independent of frequency.

3.2.2.a - Estimation of the Amplitude and Frequency of Oscillation

To provide reasonable estimate of the frequency and the amplitude of oscillation to be used as initial guess for the harmonic balance method the following simplified approach is performed.

The simplified equivalent version of a negative conductance oscillator is shown in Fig. (3-7)



Fig(3-7): A negative resistance oscillator

This study is based on the assumption that only the fundamental frequency appears across the diode's terminals and all the higher harmonics are shorted out. Through this analysis we can determine an approximate value for the oscillation

frequency and the amplitude of oscillation. We shall use this approximate solutions as the initial guess for the harmonic balance analysis.

In the stable state, the admittance across the terminals x-x in Fig.(3-7) seen in one direction should be equal to the negative of the admittance seen in the other direction.

The nonlinear admittance of the diode is given by

$$Y_d = -G_0(1 - \alpha V_d^2) + j\omega C_{d0}(1 + \beta_d^2) \quad (3-21)$$

where V_d is r.m.s value of the voltage across the diode's terminals. To satisfy the requirements for steady state oscillation:

$$G_0(1 - \alpha V_d^2) = G_l \quad (3-22)$$

$$-\omega C_{d0}(1 + \beta V_d^2) = \omega C_p - 1/\omega L_p \quad (3-23)$$

The power generated by the diode is given by

$$P = G_l V_d^2 = G_0(1 - \alpha V_d^2) V_d^2 \quad (3-24)$$

In order to get the maximum output power, we differentiate the Eq.(3-24) with respect to V_d^2 and equate it to zero to get

$$\alpha = \frac{1}{2V_m^2} \quad (3-25)$$

where V_m is the rms voltage that yields the maximum power. Substituting Eq.(3-25) into Eq.(3-24) we get an expression for maximum output power.

$$P_m = \frac{1}{2} G_0 V_m^2 \quad (3-26)$$

The normalized power can be expressed as

$$P_n = \frac{P}{P_m} = \frac{G_l V_d^2}{\frac{1}{2} G V_m^2} = 2 g_l v_d^2 \quad (3-27)$$

where

$$g_l = \frac{G_l}{G_0} \quad (3-28)$$

and

$$v_d = \frac{V_d}{V_m} \quad (3-29)$$

Using Eqs. (3-22) and (3-25) we get

$$g_l = 1 - \frac{1}{2} v_d^2 \quad (3-30)$$

By combining Eqs. (3-27) and (3-30) we get

$$P_n = 4g_l(1 - g_l) \quad (3-31)$$

This equation shows the dependence of the power on the load. The highest power is obtained when $g_l = \frac{1}{2}$ or

$$G_l = \frac{1}{2}G_0 \quad (3-32)$$

This shows in order to get the maximum power the conductance of the load should be half the small signal conductance of the diode.

The oscillation frequency may be obtained from Eq.(3-23). If the amplitude of voltage across the diode's terminals is small,

$$\omega_0 = \frac{1}{\sqrt{L_p(C_{do} + C_p)}} \quad (3-33)$$

The oscillation frequency is decreased with increasing voltage across the diode.

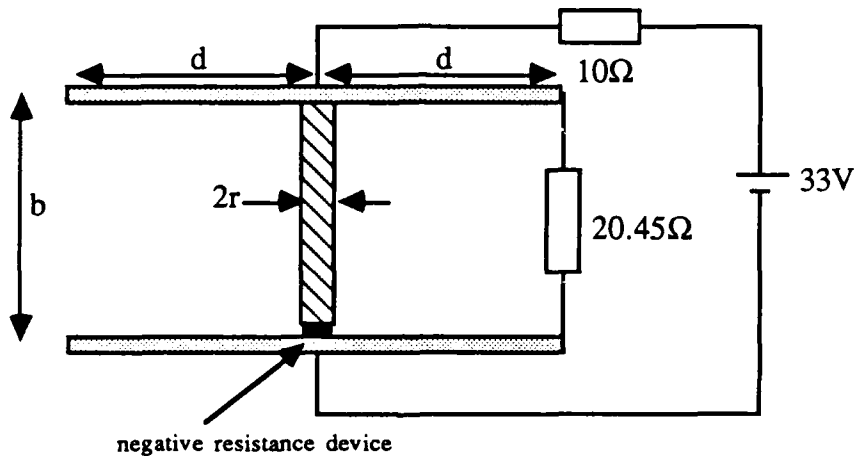
3.2.2.b - The Harmonic Balance Results

A sample problem is designed to test the nonlinear analysis program. A negative conductance diode is inserted in a parallel plate waveguide. The I-V characteristic for the test diode is

$$I = 0.01(V - 3.0)^3 + 8.56 \times 10^{-2} (V - 3.0) + 3.0 \quad (3-34)$$

where $a_1 = 8.56 \times 10^{-2}$ and $a_3 = 0.01$, therefore the small signal negative conductance $G_0 = 8.56 \times 10^{-2}$. In the test case it is assumed that the junction capacitance C_d is frequency

and level independent. The value of C_d is chosen to be equal to 0.1 pF. For the analysis the C_d is embedded in the linear part of the circuit. By comparing Eq.(3-24) with Eqs.(3-17) and (3-18) $\alpha = 0.175$. In order to obtain maximum power the resistance of the load seen by the diode should be equal to 23.4Ω . Based on the small signal analysis the following oscillator circuit is designed to oscillate at frequency 75.3 GHz.



Fig(3-8): A negative resistance oscillator

$$b(\text{height}) = 0.254$$

$$a(\text{width}) = 0.254$$

$$d = 0.815$$

$$Z_1 = 20.45 \text{ ohms}$$

$$I_{\text{bias}} = 10.0 \text{ ohms}$$

$$V_{\text{bias}} = 33.0 \text{ volts}$$

Based on the simplified nonlinear analysis that was explained in the last section the initial guess for the amplitude of oscillation in the above case is calculated to be about 2.4 volts peak. (using Eq. 3-25) Also the resonance frequency of the linear circuit is 75.3 GHz.

After performing the harmonic balance analysis on the above circuit the following results are obtained.

Number of harmonics considered across the diode's terminals: 5

Initial guess for the oscillation frequency: 75.3 GHz

Initial guess for the amplitude of the fundamental component: 2.4 volts

Results after convergence:

$$V_{dc} = 3.0 \text{ volts}$$

$$\text{Frequency of oscillation} = 74.39 \text{ GHz}$$

Voltage components across the diode's terminals:

N	Amplitude (volts)	Phase(radians)
1	2.4137	0.0
2	2.99×10^{-4}	1.74
3	0.1746	1.98
4	7.649×10^{-4}	-2.07
5	3.72×10^{-2}	-2.48

It can be seen that due to generation of higher harmonics the oscillation frequency is lower than the resonance frequency of the linear circuit. The frequency shift is small (about 1.2%) due to the fact that it is a second order effect. Also the

amplitude of the fundamental frequency of oscillation is very close to the expected value.

To check the convergence of the analysis we chose a different initial guess and run the program again.

Number of harmonics considered across the diode's terminals: 5

Initial guess for the oscillation frequency: 76.0 GHz

Initial guess for the amplitude of the fundamental component: 6.0 volts

Results after convergence:

$$V_{dc} = 3.003 \text{ volts}$$

$$\text{Frequency of oscillation} = 74.395 \text{ GHz}$$

Voltage components across the diode's terminals:

N	Amplitude (volts)	Phase(radians)
1	2.4132	0.0
2	9.0×10^{-4}	-0.511
3	0.17487	2.088
4	2.659×10^{-3}	-2.185
5	4.06×10^{-2}	-2.324

The initial guess for the amplitude of oscillation is bigger than twice the final value. Convergence to the same amplitude occurs with the initial values chosen to be smaller than the true value. This proves the existance of a stable limit cycle with an amplitude of 2.41 volts. Of course if the value of the initial guess is too small then the amplitude will converge to zero which is also a stable focus (No oscillation). Unfortunately the

harmonic balance method does not give us any insight about the build up of oscillation, because that is a transient phenomenon. In the design of oscillators one should be sure that the oscillation's start up conditions are satisfied [12].

3.3 - Large Signal Analysis of A QWITT Qscillator

Using the harmonic balance method the large signal analysis of the QWITT diode oscillator is performed. The analysis is similar to the one in test #2. The only difference is that the subroutine NONLINEAR contains the large signal model of the QWITT diode. As before the QWITT diode is inserted in a parallel plate waveguide via an inductive post. The nonlinear analysis is performed considering only one harmonic across the QWITT diode. Due to the fact that the amplitudes of the higher harmonics are much smaller than the amplitude of the fundamental frequency of operation, neglecting higher harmonics will not have much effect on the accuracy of our analysis. The large signal analysis is performed only for a single diode oscillator.

3.3.1 - Large Signal Model of The QWITT

We want to find the current through the QWITT diode as a function of dc bias, ac voltage at the fundamental frequency across the diode, and frequency of operation..The large signal diode model [13] uses a piecewise linearized fit to an experimental dc IV characteristic of the quantum well to describe current injection. Using the Ramo-Shockley theorem for transit time effects, a numerical integration of the injected charge pulse over the entire rf cycle is performed to obtain the device current. The electric field and the carrier velocity in the drift region are assumed to be constant. Static quantum well I - V characteristics are assumed to be valid at all frequencies. Fourier analysis of the device current gives the device conductance and susceptance per unit area.

First we need to find an expression for the total current density as a function of injection angle θ . Consider that a particle is injected at an angle θ from the quantum well device into the drift region. If we assume that the electric field in the drift region is strong enough (high bias voltage) then the particle's velocity in the drift region can be assumed to be equal to the saturation velocity of electrons v_s in that region. By the time the particle reaches the contact at the end of the drift region, its phase angle will be $\theta + \theta_c$ where θ_c is the drift angle of the drift region. At angle θ all particles injected from $\theta - \theta_c$ up until θ are still drifting through the device. We can write

$$Q(t) = \int_{\theta - \theta_c}^{\theta} J_{QW} dt \quad (3-35)$$

where

$Q(t)$ = Total charge drifting through the device at time t .

$J_{QW}(t)$ = Particle current density through the quantum well at time t .

It is assumed that $J_{QW} = J_{QW}(V_{QW})$ is a known J-V characteristic and that the transient J-V characteristic is approximately equal to the steady state J-V characteristic.

We can change the integration variable

$$\frac{\theta}{2\pi} = \frac{t}{T} = f.t$$

so

$$dt = \frac{1}{2\pi f} d\theta$$

where f is the frequency of operation. Eq.(3-35) can be written

$$Q(\theta) = \frac{1}{2\pi f} \int_{\theta-\theta_s}^{\theta} J_{QW}(\theta') d\theta' \quad (3-38)$$

By the Ramo - Shockley theorem, we can write

$$J(\theta) = \frac{Q(\theta) \cdot v_s}{W} \quad (3-39)$$

where

v_s = saturation velocity of electrons in the drift region

W = drift region's length

From Eq.(3-38) and Eq.(3-39) we can write

$$J(\theta) = \frac{v_s}{2\pi f W} \int_{\theta-\theta_s}^{\theta} J_{QW}(\theta') d\theta' \quad (3-40)$$

and since $\frac{2\pi}{\lambda} W = \theta_d$ and $\lambda = \frac{v_s}{f}$ we get

$$W = \frac{\theta_d v_s}{2\pi f} \quad (3-41)$$

therefore by substituting Eq.(3-41) into Eq.(3-40) the following is obtained

$$J(\theta) = \frac{1}{\theta_d} \int_{\theta-\theta_s}^{\theta} J_{QW}(\theta') d\theta' \quad (3-42)$$

Given $J_{QW}(V_{QW})$ one can calculate $J(\theta)$ by numerical integration of $J_{QW}(V_{QW}(1 + \gamma \sin(\theta)))$ where it is assumed that

$$V = V_0(1 + \gamma \sin(\theta)) = \text{total voltage across device} \quad (3-43)$$

$$V_{QW} = V_{QW}^{dc}(1 + \gamma \sin(\theta)) = \text{voltage across quantum well} \quad (3-44)$$

where

V_0 = the dc voltage across the QWITT

γ = ac modulation factor

and

$$V_1 = V_0\gamma \sin(\theta) \quad (3-45)$$

where V_1 is the ac voltage component at the fundamental frequency.

$$J_1(\theta) = J_{1s} \sin(\theta) + J_{1c} \cos(\theta) \quad (3-46)$$

where $J_{1\theta}$ is the ac component of current at the fundamental frequency. We can find J_{1s} and J_{1c} from Fourier analysis.

$$J_{1s} = \frac{1}{\pi} \int_0^{2\pi} J(\theta) \sin(\theta) d\theta \quad (3-47)$$

$$J_{1c} = \frac{1}{\pi} \int_0^{2\pi} J(\theta) \cos(\theta) d\theta \quad (3-48)$$

from Eq.(3-42), (3-47) and (3-48) we get

$$J_{1s} = \frac{1}{\pi \theta_d} \int_0^{2\pi} \sin(\theta) \left(\int_{\theta=0}^{\theta} J_{QW}(\theta) d\theta \right) d\theta \quad (3-49)$$

$$J_{1c} = \frac{1}{\pi \theta_d} \int_0^{2\pi} \cos(\theta) \left(\int_{\theta=0}^{\theta} J_{QW}(\theta) d\theta \right) d\theta \quad (3-50)$$

3.3.2 - Results of Harmonic Balance Analysis

The large signal conductance and susceptance as a function of frequency for a QWITT diode (10 μm diameter) operating in the $\frac{3\pi}{2}$ mode is shown in Fig.(3-9). As one can see the negative conductance of the diode decreases with increasing frequency. Also the susceptance of the QWITT which is due to the parallel capacitance of the diode increases as frequency increases. These two effects both reduce the efficiency of the diode at very high frequencies.[14]

The plot of the output power of a QWITT oscillator as a function of frequency is shown on Fig.(3-10). The length of the drift region is optimized to generate maximum power at each frequency. The linear part of the circuit was designed to match the diode impedance perfectly. As shown the power decreases with frequency increase.

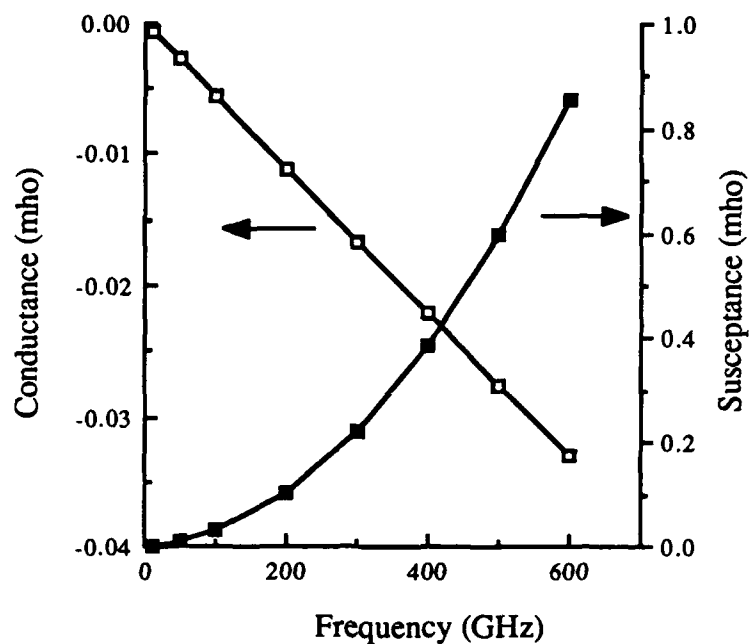


Fig.(3-9): Large signal conductance and susceptance as a function of frequency for a QWITT diode(10 mm diameter) operating in the $\frac{3\pi}{2}$ mode.

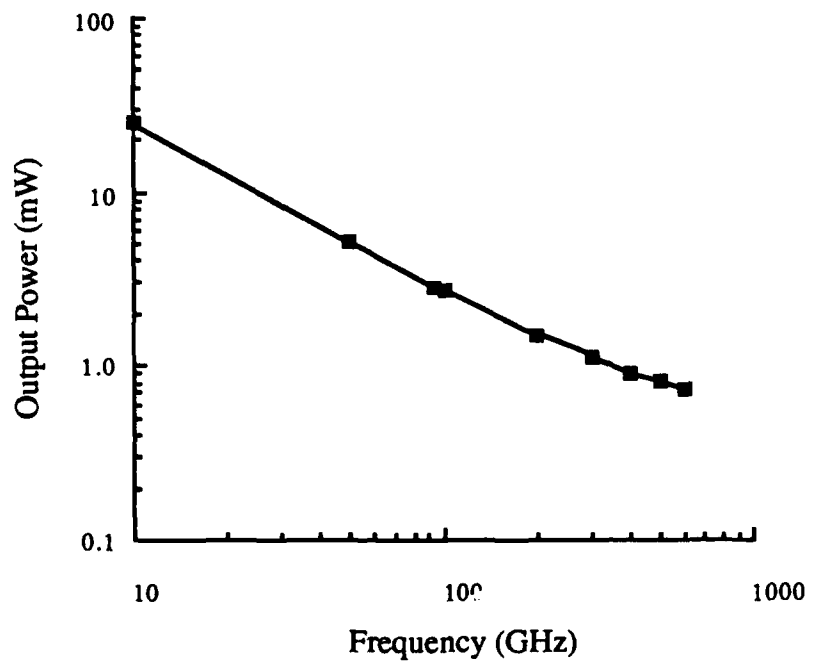


Fig.(3-10): Output power as a function of frequency for a single QWITT diode

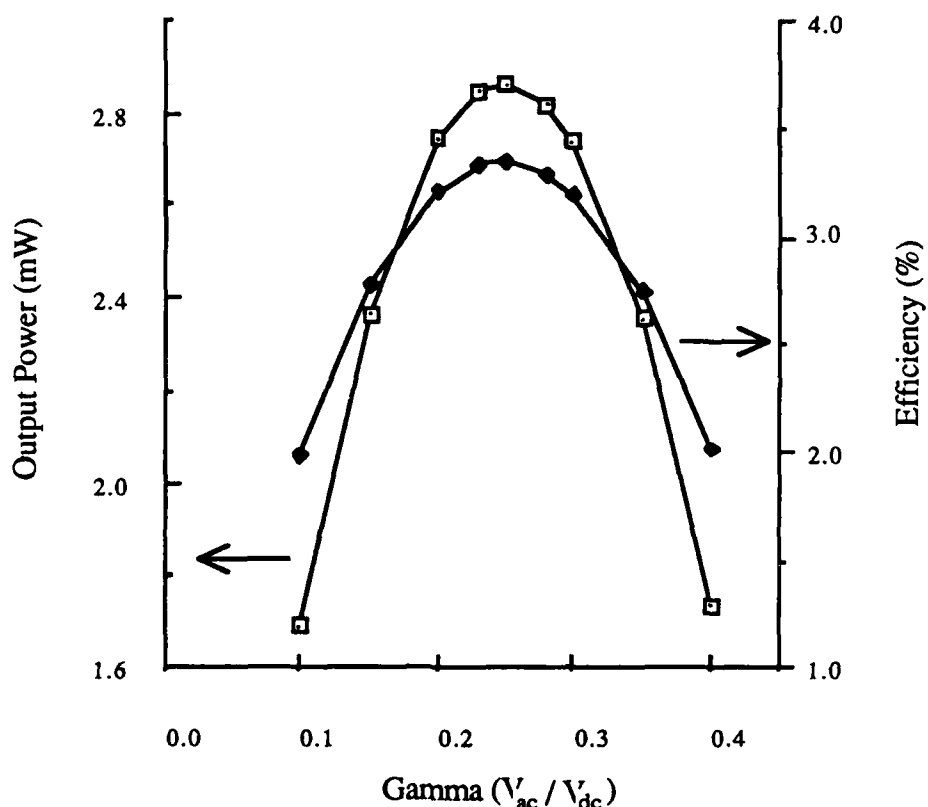


Fig.(3-11): Output power and efficiency as a function of gamma

On Fig.(3-11) the plot of output power and efficiency as a function of the ratio of the ac to the dc voltage (gamma) across the diode is shown. The oscillation frequency is 94 GHz. At each gamma point an optimum load is used for maximum power generation. It is clear that there is an optimum ac modulation across the diode for maximum power generation. As the amplitude of the ac voltage across the diode increases the impedance of the diode changes (the negative conductance decreases) and that causes the power to drop from its optimum value.

Chapter 4

EXPERIMENT

Two experiments were performed to demonstrate the oscillation capability of the QWITT at microwave frequencies. For both experiments QWITT diodes with different drift region length were used to determine the dependence of the power generated on the drift region lengths. The power obtained at different frequencies was lower than the maximum theoretically predicted power for the QWITT diode. The physical structure of the device is shown on Fig.(4-1) [15]

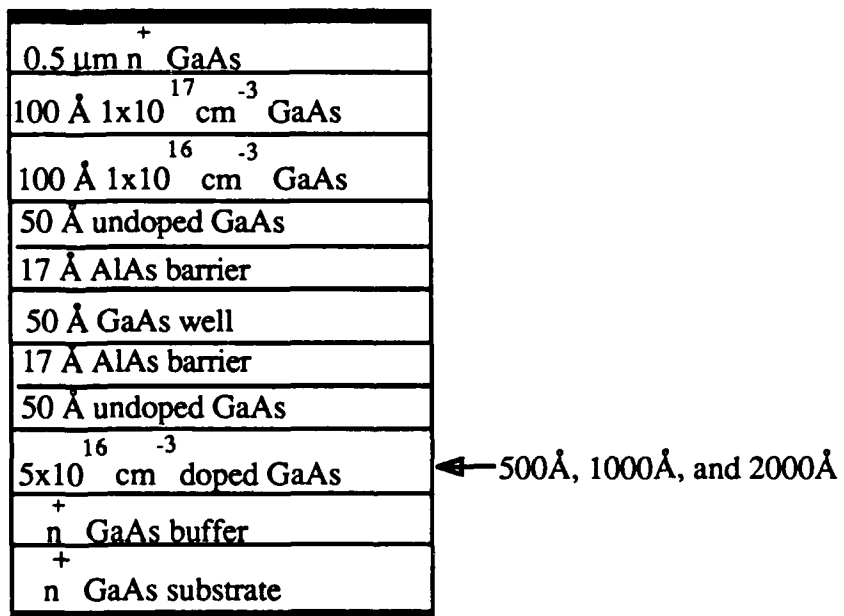


Fig.(4-1): physical structure of the QWITT

4.1 - QWITT Diode In A Rectangular Waveguide

Three different QWITT diodes with drift regions 500A, 1000A and 2000A were examined. Devices had a nominal area of $3.3-3.8 \times 10^{-7}$ cm 2 with a height of around

0.5 μm . The devices were mounted in a WG-16 (8.2 - 12.4 GHz) waveguide using a micrometer controlled post and a whisker contact. One side of the waveguide was connected to a tunable short (Fig. 4-2) The frequency of the oscillator could be adjusted by varying the position of the short and the bias voltage.

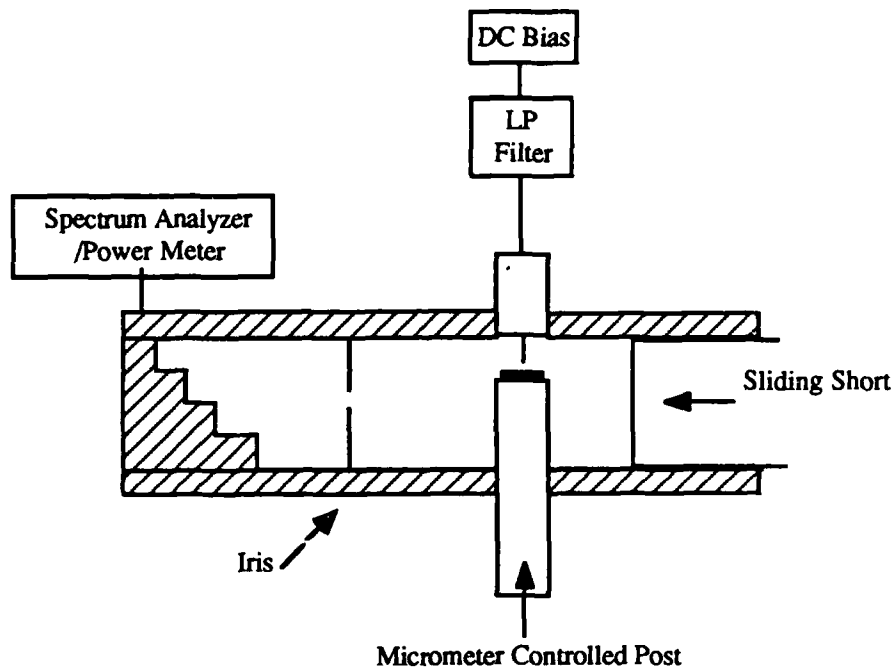


Fig.(4-2): waveguide oscillator using QWITT diode

The rf performance of three diodes is given in table (4-1). The output powers obtained were less than the theoretically predicted values. This may be due to the fact that the impedance of the diode was not matched to the characteristic wave impedance of the full height waveguide. The maximum power was obtained using a device with the drift region length of 2000A which is very close to the $\frac{3\pi}{2}$ mode of operation at 10 GHz

Length of Drift Region (Å)	Specific Negative Resistance (10^5 Ohm-cm 2)	Output Power (μW)	Oscillation Frequency (GHz)
500	2.6	3	10.2
1000	4.9	10	10.4
2000	19	30	10.6

Table (4-1)

4.2 - Planar Structure

The QWITT diodes were mounted on a planar microstrip structure. The maximum power obtained was about 900 μW at 4.2 GHz. One reason for obtaining higher power using the planar circuit is that the impedance of the diode is better matched to the impedance of the microstrip structure. As in the case of the waveguide oscillator, here the maximum power was obtained with the diode with 2000Å drift region length. The rf performance of the planar structure is given in table (4-2).

Length of Drift Region (Å)	Specific Negative Resistance (10^{-5} Ohm-cm 2)	Output Power (μW)	Oscillation Frequency (GHz)
500	2.6	240	10.0
		275	7.0
2000	19	910	4.2

Table (4-2)

Chapter 5

Conclusion

We have applied small and large signal models for the QWITT diode in order to prove its feasibility for use in millimeter and submillimeter wave oscillators. Small signal analysis was applied to a periodic power combining structure to determine the design parameters and oscillation frequency of the oscillator. The large signal analysis for a single QWITT diode oscillator used the piecewise harmonic balance method to determine the precise amplitude and frequency of oscillation. The calculations showed that the QWITT diode is capable of producing about 1 mW power at frequencies up to 600 GHz. Furthermore an experiment was performed which verified the capability of the QWITT diode for the generation of microwave power.

Future experiments are planned which will demonstrate operation at higher power and higher frequencies. Also a periodic power combining structure will be fabricated to increase output power of the oscillator.

REFERENCES

- [1] E.R. Brown, T.C.L.G. Sollner, W.D. Goodhue, C.D. Parker, "Resonant oscillations upto 200 GHz", IEEE Dev. Res. Conf., VIA-2, Santa Barbara, California, June 1987
- [2] M.S. Nakhla, J. Vlach, "A Piecewise Harmonic Balance Technique for Determination of Periodic Responce of Nonlinear Systems", IEEE CAS-23, No.2, pp. 85-91, February 1976
- [3] L. Lewin, "Theory of Waveguides", New York, Halsted Press 1975
- [4] Y. Fukuoka and T. Itoh, "Millimeter Wave Traveling Wave IMPATT diode", Microwave Laboratory Report, University of Texas at Austin, May 1984
- [5] V.P. Kesan, D.P. Neikirk, P.A. Blakey, B.G. Streetman, T.D. Linton, "The Influence of Transit Time Effects on the Optimum Design and Maximum Oscillation Frequency of Quantum Well Oscillators", IEEE ED-35, No.4, pp. 405-413, April 1988
- [6] V.P. Kesan, A. Mortazawi, D.P. Neikirk, T. Itoh, "Monolithic Millimetre-Wave Oscillator Using a Transmission Line Periodically Loaded by QWITT Diodes", Electronics Letters, 26th May 1988, Vol. 24, No.11, pp. 666-667
- [7] J. Obergon, "Nonlinear Analysis and Design of Microwave Circuits", Proc. of the 15th European Microwave Conf., 9th-13th, September 1985, France, pp. 1089-1094
- [8] F. Filicori, "Nonlinear Microwave Circuit Analysis Using Harmonic Balance Techniques", Proc. of the 15th European Microwave Conf., 9th-13th, September 1985, France, pp. 1104-1109
- [9] D. Weiner, J. Spina, "Sinosoidal Analysis and Modeling of Weakly Nonlinear Circuits", Van Nostrand 1981
- [10] R.G. Hicks, P.J. Khan, "Numerical Analysis of Nonlinear Solid State Device Excitation in Microwave Circuits", IEEE Vol. MTT-30, No. 3, pp. 251-259, March 1982
- [11] W.J. Cunningham, "Introduction to Nonlinear Analysis", McGraw-Hill 1958
- [12] T. Berceli, "Nonlinear Active Microwave Circuits", Elsevier 1987
- [13] V. P. Kesan, T.D. Linton, C.M. Maziar, D.P. Neikirk, P.A. Blakey, B.G. Streetman, "Power Optimized Design of Quantum Well Oscillators", 1987 IEEE International Electron Device. Meeting Tech. Dig., pp. 62-65, Dec. 6-9, 1987

- [14] A Mortazawi, V.P. Kesan, D.P. Neikirk, T. Itoh, 'Periodic Monolithic Millimeter Wave Quantum Well Oscillator", The 13th International Conf. on Infrared. and mm Wave, Honolulu, Hawaii, December 5-9, 1988
- [15] V.P. Kesan, A. Mortazawi, D.R. Miller, D.P. Neikirk, T. Itoh, B.G. Streetman, "Microwave Frequency Operation of the Quantum Well Injection Transit Time (QWITT) diode", submitted for publication in the Electronics Letters